We are IntechOpen, the world's leading publisher of Open Access books
Built by scientists, for scientists

6,900
Open access books available

185,000
International authors and editors

200M
Downloads

Our authors are among the

154
Countries delivered to

TOP 1%
most cited scientists

12.2%
Contributors from top 500 universities

WEB OF SCIENCE™

Selection of our books indexed in the Book Citation Index in Web of Science™ Core Collection (BKCI)

Interested in publishing with us?
Contact book.department@intechopen.com

Numbers displayed above are based on latest data collected.
For more information visit www.intechopen.com

2

Theoretical Model of the Physical System: Optimization by the Genetic Algorithm

Stanislav Jurečka
University of Žilina
Slovakia

1. Introduction

Present state in investigation of complicated physical systems is connected in many cases with the numerical analysis of studied phenomena. Equations used for the description of given system are often complicated and have to be modified very often to reach adequate coincidence with observed behaviour of modeled system. Constructed theoretical model contains a lot of assumptions, it tries to describe various influences connected with his own structure as well as with interactions of given system with his environment. In consequence of this model complexity the searching for reliable and comfortable techniques for studying these systems is important. In our approach a theoretical model of physical system is constructed in two steps. Initial estimation of model parameters is performed in graphical user interface and obtained theoretical model is then refined by the genetic algorithm. This enables comfortable realization of changes in theoretical model, implementation of subjective decisions and restrictions as well as controlled refinement of searched model parameters. In this chapter we use this approach for study of optical properties of multilayer system.

2. Optical properties of solids

Detailed knowledge of the optical properties of materials and structures are important for a number of industrial and research applications, especially for optoelectronics, photovoltaics, optical communications, senzorics, laser technology and so on. Optical properties are studied by analysis of light and matter interactions. The phenomena that occur while light propagates through an optical medium can be classified into several groups. The simplest are reflection, propagation and transmission. Some of the light beam incident on an front surface of the medium is reflected, while the rest enters the medium, propagates through it and can reach the back surface of the media. Here it can be reflected again, or it can be transmitted through to the next medium. When a light propagates through the optical medium several other phenomena occur: refraction, luminiscence, scattering and if the intensity of the beam is very high other nonlinear phenomena can occur.
Refraction causes the light waves propagate with a smaller velocity than in free space. Refraction does not affect the intensity of the light wave.
Absorption occurs if the frequency of the light is resonant with the transition frequencies of the atoms in the medium. The light beam is attenuated as it progresses in this case. The

transmission of the medium is therefore related to the absorption, selective absorption is responsible for the colouration of material.
Luminiscence denotes all processes connected to the spontaneous emission of light by excited atoms in a solid state material. It can accompany the propagation of light in an absorbing medium, light is emitted in all directions and contains the different frequencies.
During *scattering* the light changes direction and possibly also its frequency after interacting with the medium. The total number of photons is unchanged but the light is redirected in other directions.

2.1 The complex refractive index

The optical phenomena described above can be quantified by several parameters that determine the properties of the medium at the macroscopic level. The reflection at the surface is described by the reflectivity *R* and is defined as the ratio of the reflected power to the power incident on the surface. The propagation of the light through the medium is described by the refractive index *n*, defined as the ratio of the velocity of light in free space to the velocity of light in the medium. The refraction index depends on the frequency of the light. This is called *dispersion*. The absorption of light by an optical medium is described by its *absorption coefficient* α. According to the Beer's law the intensity of light (optical power per unit area) at position *z* in the propagation direction is given by the equation

$$I(z) = I(0)e^{-\alpha z} \tag{1}$$

The absorption coefficient strongly depends on frequency. The absorption and the refraction can be incorporated into a single quantity called complex refractive index $\tilde{n}$

$$\tilde{n} = n + i\kappa \tag{2}$$

The real part of complex refractive index is refractive index *n* and the imaginary part κ, called the extinction coefficient, is directly proportional to the absorption coefficient α of the medium

$$\alpha = \frac{4\pi\kappa}{\lambda_0} \tag{3}$$

where λ_0 is the free space wavelength of the light. We can relate the complex refractive index to the complex relative dielectric constant $\tilde{\varepsilon}_r = \varepsilon_1 + i\varepsilon_2$

$$\begin{aligned} n &= \sqrt{\varepsilon_1} \\ \kappa &= \frac{\varepsilon_2}{2n} \end{aligned} \tag{4}$$

The microscopic models usually enable calculation of complex dielectric function. The measurable optical parameters are then determined by converting ε_1 and ε_2 to *n* and κ. The reflectivity *R* of given surface depends on both *n* and κ. Reflectivity between the medium and the vacuum at normal direction is given by

$$R = \left|\frac{\tilde{n}-1}{\tilde{n}+1}\right|^2 = \frac{(n-1)^2+\kappa^2}{(n+1)^2+\kappa^2}. \tag{5}$$

In a transparent material in the visible region of the spectrum, the absorption coefficient is very small, ε_2 and κ values are neligible. If there is significant absorption, then we need to know both the real and imaginary parts of $\tilde{n}$ and $\tilde{\varepsilon}$.

2.2 Thin film system

Thin film systems are widely used in various branches of applied research and industry. Analytical expressions describing the spectral dependencies of the optical parameters of the thin film have important applications in semiconductor devices development. Such analytical expressions can be used to analyse optical data and extract material parameters. The values of parameters deduced from the optical experiment include the atomic oscillator properties and provide information on composition and microstructure of the sample. To be able to determine the optical properties of the thin film system in a wide spectral region an adequate microstructural and physical model of this system have to be created. Spectral dependencies of the optical quantities depend on the electronic structure and existing bonds and thus provide information useful for the material structure and its properties understanding. A lot of consideration was devoted to the gap and interface states and methods developed for their passivation are studied to increase quality of the thin film systems in the semiconductor devices.

Properties of the amorphous hydrogenated silicon (a-Si:H) samples prepared for the solar cell and TFT applications by various techniques were analysed in our laboratory. The main goals of these studies are the defect states in the thin film structure determination and improvement of the structural, electrical and optical material properties for the device construction. In this chapter a mathematical background and implementation of a new method of the optical properties of the thin film system analysis is presented. Optical properties of the thin film system are determined by computer modeling of the optical transitions connected with the electronic states. The properties of the developed method as well as experimental results obtained by analysis of the experimental spectral reflectance of the a-Si:H samples will be described.

The interaction of photons and matter is explained by quantum electrodynamics. Adequate description of this interaction for the purposes of the optical properties analysis can be also obtained by using the classical theory of electricity and magnetism. The wavelength of light wave λ in material is determined by

$$\lambda = \frac{2}{\sqrt{\mu\varepsilon}\,\omega}, \tag{6}$$

where ω is the angular frequency, μ is the permeability and ε is the permitivity of the material. Both μ and ε depend on the medium properties and therefore the wavelength depends on the material the light is propagating through.

Electron can be considered as harmonic oscillator coupled to a fixed nucleus. The electron - nucleus interaction is modeled by a spring force that implies a harmonic oscillator frequency ω_0. A physical motivation of the spring force model is the coulombic force that binds the electron to the nucleus. There is also a damping force that is proportional to the velocity of

the electron movement. The frequency that the electron moves depends on the distance from the nucleus. The distance of the electron from the nucleus is related to the energy of the electron state. The nucleus is assumed to be fixed and motionless and does not interact with photons. Each electron in an atom has a resonating frequency ω_0 that is associated with the energy of the electron state.

The interaction of photon with frequency ω and a single electron with an oscillating frequency ω_0 can be described by Maxwell's equations. The displacement of the electron by the electric field component of the light creates a dipole moment in the atom. The time-dependent dipole moment $\tilde{p}(t)$ created by the movement of the electron is

$$\tilde{p}(t) = \frac{e^2}{m_e\left(\omega_0^2 - \omega^2 - i\gamma_j\omega\right)}\vec{E}_0\, e^{-i\omega t} \tag{7}$$

where m_e is the mass of an electron, e is the charge of an electron, γ_j is a damping factor, and $\vec{E}_0$ is the amplitude of the electric field. In real material electrons may oscillate at one of several different oscillating frequencies that are material specific. If there are N atoms per unit volume, and there is a fraction f_j of the electrons with frequency ω_j and damping factor γ_j, the complex permitivity of material takes the form

$$\tilde{\varepsilon} = \varepsilon_0\left[1 + \frac{Ne^2}{m_e\varepsilon_0}\sum_j \frac{f_j}{\omega_0^2 - \omega^2 - i\gamma_j\omega}\right]. \tag{8}$$

The term f_j is called the oscillator strength. It is the measure of how one electron contributes to the overall response of the material to the incident light wave at given frequency. The electronic structure of a material determines the energies with which the electrons are bound to the nuclei and the bonds with the surrounding atoms. The optical properties of materials in the UV region of the spectrum depend primarily on the core electrons. The bonded valence electrons do not significantly affect the inner electrons. The bonding of the valence electrons to the surrounding atoms does not significantly change the optical constants at energies above 100 eV. In the visible and infrared region the interaction of light depends on the energies of the valence electrons. The bonds of the valence electrons with valence electrons in the neighbor atoms determine the energy of valence electrons in a bulk material. The oscillator properties of the core electrons do not play significant role in this case. In the visible and IR region the optical properties are determined mainly by the states of the valence electrons in bonding orbitals. Important role play also vibrational and rotational movements of molecules. Interaction of incident electromagnetic wave with molecules leads to rotational and vibrational spectra in infrared and microwave regions.

The refractive index and the extinction coefficient are experimentally accessible by reflective and absorptive spectroscopies. Theoretical formulations of the refractive index n and the extinction coefficient κ for the semiconductor materials can be obtained from the energy-dependent dielectric function. *Jellison and Modine* derived the analytical expression for the $\varepsilon_2(E)$ function in the form

$$\varepsilon_2(E) = \frac{A E_0 \Gamma E}{E^2 - E_0^2 + \Gamma^2 E^2}\frac{\left(E - E_g\right)^2}{E^2} = L(E)G(E), \tag{9}$$

where A, Γ, E_0 are amplitude, broadening and resonance energy. E_g denotes the semiconductor band gap, E is the photon energy. The function $L(E)$ is a lineshape function and the $G(E)$ function describes $\varepsilon_2(E)$ for $E \approx E_g$. The real part of the dielectric function $\varepsilon_1(E)$ can be expressed by

$$\varepsilon_1(E) = \varepsilon_{1\infty} + K\{\varepsilon_2(E)\} = \varepsilon_{1\infty} + \frac{2}{\pi}\int_0^{\infty} \frac{s\,\varepsilon_2(s)\,ds}{s^2 - E^2} \tag{10}$$

where $\varepsilon_{1\infty}$ accounts for possible high-energy transitions and K is the Kramers-Kronig integral. Within the Jellison-Modine dispersion model the absorption connected with the localized states in the band gap of the semiconductor material is not accounted. The band-to-band transitions are only respected. To obtain better expression for the dielectric function applicable to various types of semiconductors the $G(E)$ function was modified. In the *Urbach-Tauc-Lorentz model* the imaginary part of the dielectric function $\varepsilon_2(E)$ was changed

$$G(E) = \frac{(E - E_g)^2}{E_P^2 + (E - E_g)^2} \tag{11}$$

where $E_P \approx E_g$ is a variable parameter. Function $G(E)$ in this dispersion model improves the theoretical dielectric function values for the photon energies above the band gap. The real part of the dielectric function $\varepsilon_1(E)$ is given by the Kramers-Kronig integral too.
Forouhi and Bloomer derived a formula for the extinction coefficient and the refractive index in the forms

$$n(E) = n_b + \frac{B_0 E + C_0}{E^2 - BE + C} \tag{12}$$

$$\kappa(E) = \frac{A(E - E_g)^2}{E^2 - BE + C} \tag{13}$$

where A, B, B_0, C, C_0 are model parameters. The extinction coefficient in the Forouhi-Bloomer dispersion model does not comply with *f*-sum rules. *f*-sum rules are important constraints for the analysis of optical quantities and involve all absorption processes including valence-band excitations and inner-shell ionizations over the entire energy interval. The Forouhi-Bloomer dispersion model cannot be therefore applied to photon energies above the resonant values.
Typical spectrum of the optical quantity of semiconductor material usually reveals separated peaks due to different absorption processes. For example the spectral dependency of the refractive index of crystalline silicon is in Fig. 1.
Theoretical derivations of the optical parameters dispersion relations assume zero energy breadth in the interband transitions. This assumption leads to the Dirac $\delta-$function dependence of the extinction coefficient on photon energy

$$\kappa(\omega) = \frac{\pi f_0}{4\omega_0}\left[\delta(\omega - \omega_0) - \delta(\omega + \omega_0)\right] \tag{14}$$

where f_0 is the dipole oscillator strength and ω_0 is the transition frequency. The refractive index is given by the Kramers - Kronig integral of $\kappa(\omega)$. In reality, the spontaneous emission produces the damping of excited states in agreement with the Heisenberg relations. To accommodate the damping effect, the $\delta-$functions can be replaced by the Cauchy functions.

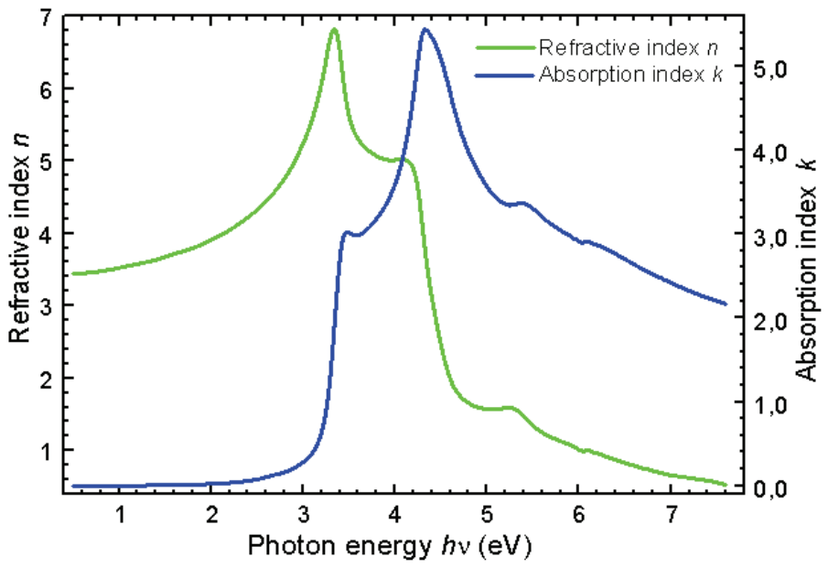

Fig. 1. Refractive index and absorption coefficient of crystalline silicon (www.ioffe.ru).

Theoretical expressions for the refractive index and the extinction coefficient after incorporating the damping effect then take the form

$$\kappa(\omega)=\sum_{i=1}^{s}\frac{f_i\Gamma_i\omega}{\left((\omega-\omega_i)^2+\Gamma_i^2\right)\left((\omega+\omega_i)^2+\Gamma_i^2\right)}, \tag{15}$$

$$n(\omega)=n_b-\frac{1}{2}\sum_{i=1}^{s}\frac{f_i\left(\omega^2-\omega_i^2-\Gamma_i^2\right)}{\left((\omega-\omega_i)^2+\Gamma_i^2\right)\left((\omega+\omega_i)^2+\Gamma_i^2\right)}. \tag{16}$$

In these equations s denotes the total number of transitions from the valence to the conduction bands, n_b is the background refractive index due to the contribution from core electrons in inner shells

$$n_b\approx 1+\frac{1}{2}\sum_{i=1}^{s}\frac{f_i}{\omega_i^2+\Gamma_i^2}. \tag{17}$$

The broadening of the spectral line describing the optical transition is in this dispersion model expressed by the Cauchy function (Chen et al., 1993).

A computation of the spectral reflectance for a plane electromagnetic wave incident upon a multilayer structure can be described by Fig. 2. In a case of a finite number of homogeneous and isotropic layers the determination of the theoretical spectral reflectance is efficient for

the experimental reflectance interpretation and enables spectral dependencies of the optical parameters calculations. For the optical field of the layered media calculations the matrix method is usually applied (Abeles, 1950; Lekner, 1987).

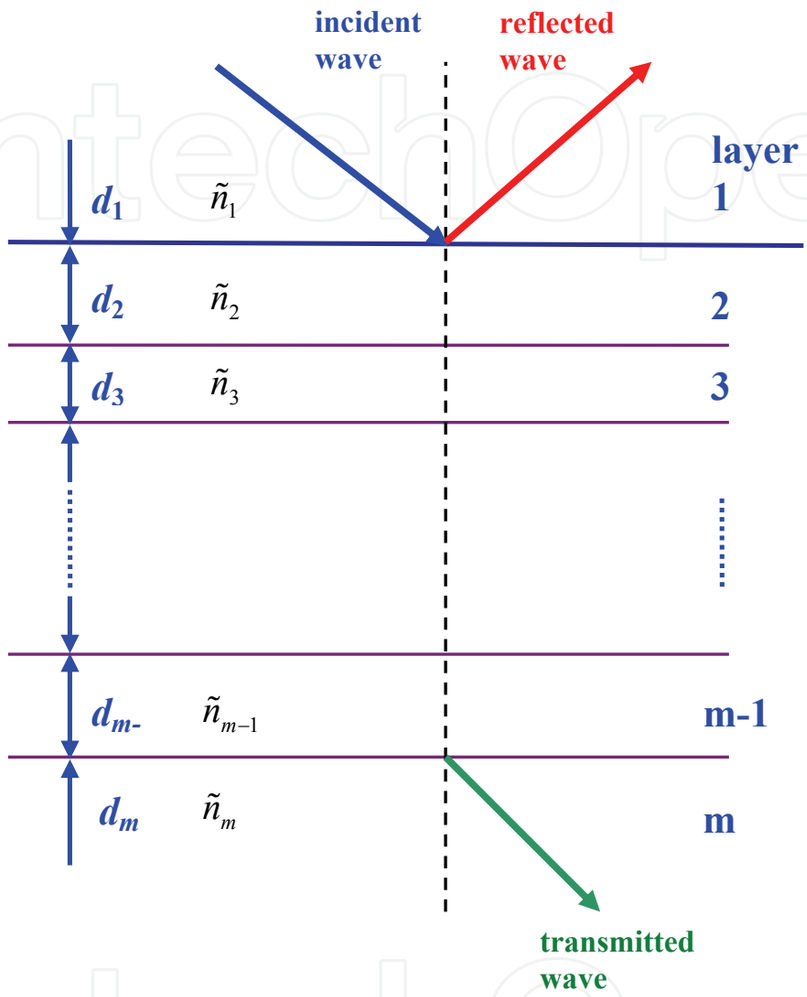

Fig. 2. Waves reflected and transmitted by a multilayer system.

The matrix procedure for calculating the reflectance from multilayers in transverse electric (TE) mode uses convention shown in Fig. 3.

Similar convention is used for the transverse magnetic TM mode. The TE reflection coefficient is given by

$$r_{TE} = \frac{E_R}{E_i} = \frac{(m_{00} + m_{01}p_m)p_1 - (m_{10} + m_{11}p_m)}{(m_{00} + m_{01}p_m)p_1 + (m_{10} + m_{11}p_m)} \tag{18}$$

where m_{xx} are the elements of the matrix M

$$M = \begin{pmatrix} m_{00} & m_{01} \\ m_{10} & m_{11} \end{pmatrix} = \prod_{i=0}^{m-1} M_i \tag{19}$$

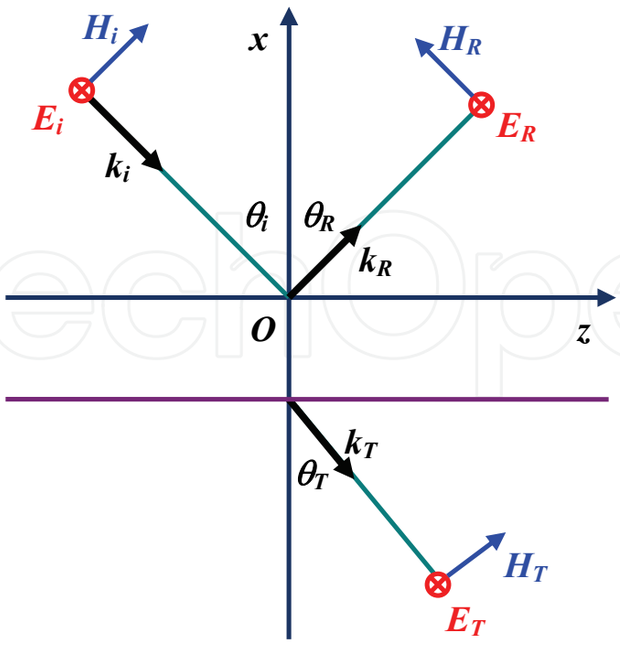

Fig. 3. Description of TE mode. *I-incident wave, R reflected wave, T- transmitted wave.*

where

$$M_k = \begin{pmatrix} \cos\beta_k & -\frac{i}{p_k}\sin\beta_k \\ -i\,p_k \sin\beta_k & \cos\beta_k \end{pmatrix} \tag{20}$$

$$\beta_k = \frac{2\pi}{\lambda} n_k d_k \sqrt{\mu}\cos\theta_k \tag{21}$$

$$p_k = \begin{cases} \sqrt{\frac{\varepsilon_0}{\mu}}\, n_k \cos\theta_k, & \text{TE mode} \\ \sqrt{\frac{\varepsilon_0}{\mu}}\, n_k \cos\theta_k, & \text{TM mode} \end{cases} \tag{22}$$

and the subscript k denotes the layer number (Hecht, 2002; Born & Wolf, 2002; Furman & Tikhonravov, 1992). The spectral reflectance is then defined by

$$R = |r_{TE}|^2 = r_{TE}\, r_{TE}^* \tag{23}$$

for TE mode or

$$R = |r_{TM}|^2 = r_{TM}\, r_{TM}^* \tag{24}$$

for TM mode. The spectral transmittance can be derived by the similar way.

2.3 The inhomogeneity of the layer material

Optical properties of inhomogeneous material can differ from the homogeneous media. In a multilayer structure we can observe inhomogeneous overlayers or transition layers consisting of the mix of materials of adjacent layers. A powerful way to handle the optical properties of such composite materials is the effective medium approximation (EMA) theory. Three famous EMA models can be jointly expressed by

$$\frac{\langle\varepsilon\rangle-\varepsilon_h}{\langle\varepsilon\rangle+\gamma\varepsilon_h}=\sum_j f_j\frac{\varepsilon_j-\varepsilon_h}{\varepsilon_j+\gamma\varepsilon_h} \tag{25}$$

where $\langle\varepsilon\rangle$ is the permitivity of the effective medium, ε_h is the permitivity of the host medium, ε_j and f_j is the permitivity of the j^{th} constituent and its fraction, and γ is a factor related to the screening and shape of the inclusions (for example, $\gamma=2$ for 3-dimensional spheres) (Tompkins & Irene, 2005). Within the structure of this equation the three EMA models are:

- Lorentz-Lorentz: $\varepsilon_h=1$, where the host material is air. This EMA model assumes that the individual constituents are mixed on the atomic scale. Real materials tend to be mixed on a larger scale and therefore this model is of limited usefulness.
- Maxwell-Garnett (MG): $\varepsilon_h=\varepsilon_l$, where the host material is the material that has the largest constituent fraction. MG EMA is the most realistic model when the fraction of inclusions is significantly less than the fraction of host material (Sihvola, 1993; Weiglhofer & Lakhtakia, 2003).
- Bruggemann: $\varepsilon_h=\langle\varepsilon\rangle$, where the host material is just the effective dielectric function. The Bruggemann EMA makes no assumption concerning the material that has the highest constituent fraction. It is very useful when no constituent forms a majority of the material. It can be used for modeling the surface roughness by using a mix of approximately 50% voids and 50% host material.

When applying the EMA model for computation of optical properties one has to pay attention to the limitations of individual EMA model. More sophisticated models take into account the multiple scattering theories, statistical distributions of densities of scatterers as well as the finite-size effects of the scatterers. For most of these expressions the MG EMA is found to be the limiting case as the size of the inclusions goes to zero. The Monte Carlo simulations for configurations that correspond to random defects in periodic composite materials and investigate the role of multiple scattering and the influence of the statistical distribution of scatterers show that the MG EMA model remains accurate also at very high density of scatterers (Mallet et al., 2006).

The complications with the multivalued inversion of a complex functions in the EMA models can be avoided by re-parametrization of Eq. (25) due to (Roussel et al., 1993). The effective value of the permitivity is in this EMA model given by

$$\langle\varepsilon\rangle=z\sqrt{\varepsilon_1\varepsilon_2} \tag{26}$$

where

$$z = b + \sqrt{b^2 + 0.5}$$
$$b = \frac{1}{4}\left[(3f_2 - 1)\left(\frac{1}{p} - p\right) + p \right]. \quad (27)$$
$$p = \sqrt{\frac{\varepsilon_1}{\varepsilon_2}}$$

2.4 Visual modelling and stochastic optimization (VIMSO) method

Determination of the optical properties of multilayer structure consists, in our approach, of constructing of appropriate structural and physical model and of fitting this model to the experimental data. The theoretical model of the spectral reflectance SR is estimated and refined in steps depicted in Fig. 4.

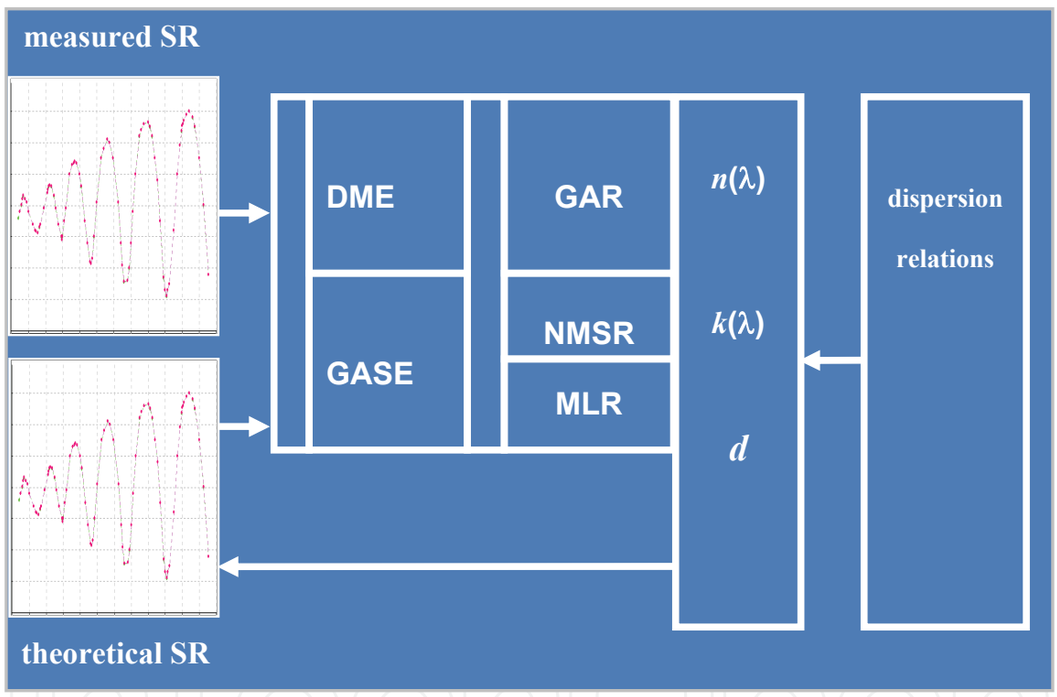

Fig. 4. Construction of theoretical model of spectral reflectance.

In this scheme DME is the visual modeling step used for the dynamic estimation of initial values of the theoretical model parameters, GASE is genetic algorithm search of these initial values, GAR is the genetic algorithm refinement step, NMSR and MLR are Nelder-Mead simplex method and Marquard-Levenberg optimization method used for the refinement of initial estimation. Implementation details of NMSR and MLR methods are not involved in this chapter. In the dispersion relations part the number of layers is fixed, and basic structure concerning the contents of each layer is set – material, thickness and homogeneity model. The dispersion relations describing the spectral behaviour of optical quantities for individual layers are defined. Here existing experimental data sets or suitable parametrization of the dispersion model are used. The last step consists of the optimization process. Here we need to estimate the values of model parameters, estimate the errors and

obtain a suitable measure of goodness of fit. Resulting theoretical model describing the spectral reflectance of multilayer structure contains a lot of unknown parameters. We divided the process of determination of the optical properties into two procedures. The first step consists of visual estimation of the structural model, dispersion relations of the optical parameters and the initial estimation of values of constructed theoretical model parameters. In the following step the values of parameters of theoretical model estimated in previous procedure are refined by the genetic algorithm. We used this approach also for solving problems in x-ray diffraction analysis (Jurečka et al., 2004), in analysis of the ion transport processes in glassy electrolytes (Bury et al., 2004) and in other applications. We use an abbreviation VIMSO for this visual modeling and stochastic optimization method.

In order to make this approach to the optical properties determination more comfortable, the graphical user interface (GUI) was built. This GUI contains:

- a table with the structure of layers,
- a list of dispersion models,
- a list of EMA models,
- a list of roughness model,
- a table of fixed parameters,
- a table of values of parameters of the theoretical model,
- a table describing the environment of the GA optimization process,
- control elements for setting the values of parameters of theoretical model,
- graphs with the experimental and theoretical data,
- a goodness of fit value.

GUI layout built in the NetBeans IDE 6.7 (SUN) is in shown Fig. 5.

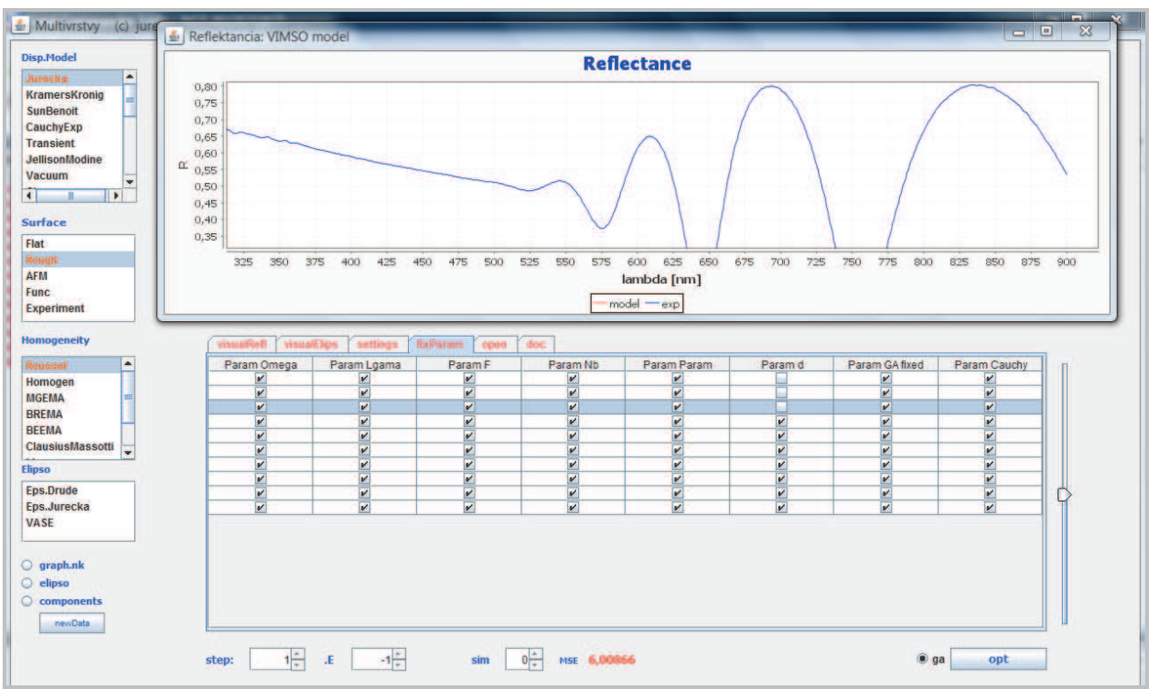

Fig. 5. GUI for determination of optical properties of multilayer structure.

In the first step of determination of the optical properties of multilayer system a suitable dispersion model is selected in a list of dispersion models. GUI structures with the dispersion models, layer homogeneity and surface roughness models are shown in Fig. 6. By selecting some cell in a column of dispersion models in a table of structure layers (see Fig. 7) the dispersion model selected in a list of dispersion models is assigned to the given layer. The same dispersion model can be assigned to several other layers in the structure.

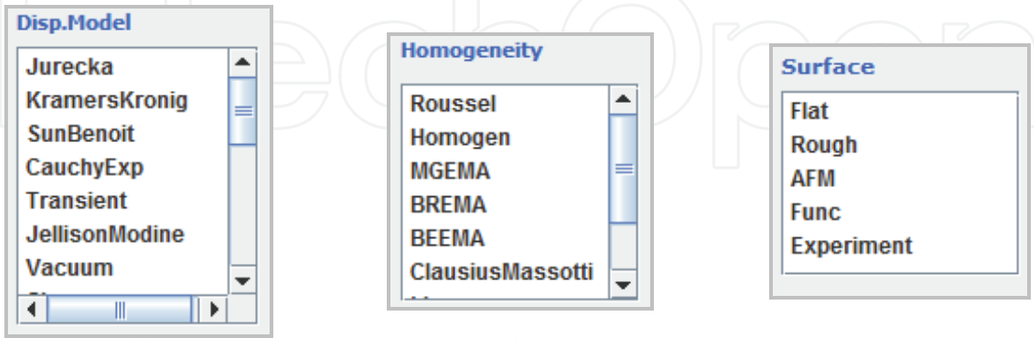

(a) (b) ©

Fig. 6. GUI structures with a) layers dispersion models, b) homogeneity models, c) surface roughness models.

Similar way of the definition of layer structure properties is used for the description of homogeneity and other structure parameters.

visualRefl | visualElips | settings | fixParam | open | doc

layer	d.model	surface	params	percentage
1 Ambient	Vacuum	Flat	Homogen	100
2 Overlayer	Jurecka	Rough	Roussel	50
3 Layer 1	Jurecka	Flat	Homogen	100
4 Layer 2	Jurecka	Flat	Homogen	100
5 Layer 3	Jurecka	Flat	Homogen	100
6 Layer 4	Jurecka	Flat	Homogen	100
7 Layer 5	Jurecka	Flat	Homogen	100
8 EMA 1	Roussel	Flat	Roussel	50
9 EMA 2	Roussel	Flat	Roussel	50
10 EMA3	Roussel	Flat	Roussel	50
11 EMA 4	Roussel	Flat	Roussel	50
12 Substrate	Si	Flat	Homogen	100
GA.iter	100	GA.elite.prob	0.1	
GA.chrom	100	GA.cross.prob.	0.25	
GA.genes	70	GA.mut.prob.	0.25	
GA.gen.len.	16	GA.cutting.prob.	0.2	
počet	901	GA.delta.par.	0.2	

Fig. 7. GUI structure with a table defining the layer structure.

In this first step the dispersion relations for individual layers are defined. According the selected layer the columns with the variables of corresponding dispersion relation are set in a table of parameters (see Fig. 8).

The value of selected parameter p can be directly written into the table cell or modified by clicking on corresponding cell of the parameters table. Parameter table mouse event listener triggers modification of clicked parameter by adding a value, defined in the control panel. Control panel contains two spinners, spinner_1 and spinner_2. Value added to the modified model parameter p' is computed by equation $p' = \pm spinner_1(value)E(\pm spinner_2(value))$.

We can study the influence of chosen theoretical model parameter onto the model behaviour

visualRefl | visualElips | settings | fixParam | open | doc

Omega	L.Gama	F	d.nm	Nb	ParamStruct	Disp.CE	Params1	Params2	Params3	x
3,43	1,51	0,6	40	1,33	1,1	5	1	1	0,5	1
3,48	0,71	5,9	500	1,33	1,1	5	1	1	0,5	2
3,72	0,476	7,2	10	1,33	1,1	5	1	1	0,08	3
4,35	0,9	1,5	20	1,33	1,1	5	1	1	0,05	4
4,75	0,88	5,5	30	1,33	1,1	5	1	1	1,8	5
5,75	3,36	21	40	1,33	1,1	5	1	1	0,8	6
6,4	8,9	23	50	1,33	1,1	5	1	1	0,5	7
7,8	25	70	60	1,33	7	5	0,6	0,04	0,5	8
10,6	3,7	70	70	1,33	1,5	5	0,3	1,8	0,08	9
23,55	9,8	0,9	0	1,33	1	5	0,3	0,8	0,05	10

Fig. 8. Table with dispersion model parameters

in a wide range of values very comfortable by this way. Alternatively we can modify selected parameter smoothly by using spinner_3. The value of this spinner defines new correction value by the equation $p'' = spinner_3 * p'$. Control panel with these spinners is shown in Fig. 5 under the structure settings table. By this way we estimate the composition of multilayer structure and initial values of theoretical model variables. When developing the structure model and estimate the parameter value the theoretical model curve and experimental data are compared graphically at a GUI panel with plots (see Fig. 5). The figure of merit of the instant theoretical model is characterized by the χ^2 value defined by the equation

$$\chi^2 = \frac{1}{N-m-1}\sum_{j=1}^{N}\left[\frac{\left(R_{\exp}\left(\lambda_j\right) - R_{theor}\left(\lambda_j, \vec{p}\right)\right)}{\sigma\left(\lambda_j\right)}\right]^2 \tag{28}$$

where N is the total number of data points, m is the number of model parameters, $R_{\exp}$ is the experimental reflectance, R_{theor} is theoretical spectral reflectance, and σ^2 is the variance of experimental data. The χ^2 value is shown at the control panel after modification of specified model parameter value. The variance limits obtained by an optimization procedure using χ^2 value is related to the actual variance limits of the fitted parameters.

3. GA optimization of theoretical model: chromosomes and fitness function

The optimization of theoretical model is complicated by the variability of suggested structure models and models of suitable dispersion relations. The number of parameters assigned for optimization is determined by the complexity of theoretical model. For optimization of theoretical model constructed and initialised in a visual modeling step of VIMSO method the genetic algorithm (Koza, 1992; Coley, 1999) is very useful. Individual parameters of theoretical model are represented by genes of the chromosome in the GA algorithm. We represented chromosome genes by the binary strings of 16 bits in our first GA implementation. The chromosome was then constructed by a concatenation of these binary strings. The number of binary strings in a chromosome was modified in accordance to proposed theoretical model. Reprogramming of the genetic operators and computation of

the chromosome fitness after changing the chromosome length is necessary too. This progress of work is laborious and requires detailed checkout. To make the procedure of the theoretical model estimation more comfortable the program packages designed for implementation of genetic algorithms enabling the object-oriented programming (Hawlitzek, 2000) are suitable. We decided to implement JGAP - a genetic algorithms and genetic programming component provided as a JAVA framework (JGAP). JGAP is designed to be flexible and modular. It is possible to create specific chromosome, genetic operators, random number generator, natural selection and other. To support these possibilities JGAP uses a Configuration object. Setting the Configuration object with all these new definitions prior running the genetic search is the first task. It is necessary to provide three extra pieces of information here: what fitness function will be used, how the Chromosomes are set and how many Chromosomes creates a population. These steps are implemented in void solveGa(.), shown in Listing 1.

Listing 1.

```
//========================================================= solveGA
 public static void solveGa(double[] parametreModelu, double[] wavelengths, double[] experimentalData, double[] sigma, boolean[] fixedParams) throws Exception
   {
      double[] Rexp = new double[wavelengths.length]; //experimental reflectance Rexp
      double[] tempE = new double[wavelengths.length]; //theoretical reflectance Rtheor
      double[] initParametre = new double[parametreModelu.length]; //model parameters
      double[] thick = new double[10]; //layer thicknesses
      int generations = (int) parametreModelu[60];
      int numchroms = (int) parametreModelu[61];
      double delta = parametreModelu[68];

     //configuration of GA environment:
      Configuration conf = new DefaultConfiguration();

     //elitism:
      conf.setPreservFittestIndividual(true);

     //instantiate & register fitness function:
      FitnessFunction fitnesFunkcia = new modelFitness(parametreModelu, wavelengths, experimentalData, sigma, fixedParams);
      conf.setFitnessFunction(fitnesFunkcia);

     //set number of genes:
      int geneCount = (int) fixedParams.length;
      for(int r=0; r<fixedParams.length; r++){
         if (fixedParams[r]) {geneCount--;}
      }
      //genecount = the number of genes, representing released parameters, max fixedParams.length
```

```
    //allocate genes:
  Gene[] mGene = new Gene[geneCount];
  int geneIndx = 0;
  for(int r=0; r< parametreModelu.length; r++){
     if (!fixedParams[r]) {
       //use structure DoubleGene(configuration, minBound, maxBound), double precision
       //delta = permitted interval for modification of suggested variable, percent
       try {
                mGene[geneIndx] = new DoubleGene(conf, parametreModelu[r]-
                delta*parametreModelu[r]/100,
                parametreModelu[r]+delta*parametreModelu[r]/100);
                geneIndx++;
       }
       catch (InvalidConfigurationException iex) {
                System.out.println("Invalid configuration: gene creation");}
      }
  }

 //instantiate model Chromosome mChromosome:
  IChromosome mChromosome;
  try {
     mChromosome = new Chromosome(conf, mGene);
   }
  catch (InvalidConfigurationException iex)
    {System.out.println("Invalid configuration: Instantiate mChromosome");}

 //register chromosome structure -> configuration
  try {
    conf.setSampleChromosome(mChromosome);
  }
  catch (InvalidConfigurationException iex)
    {System.out.println("Invalid configuration: register Chromosome");}

 //set number of Chromosomes/population
  try {
    conf.setPopulationSize(numchroms); // user defined
  }
  catch (InvalidConfigurationException iex)
    {System.out.println("Invalid configuration: Population size");}

 //seed zero population:
  Genotype population;
  population = Genotype.randomInitialGenotype(conf);//random seed

 //timing:
  long startTime = System.currentTimeMillis();
```

```
    //run GA process:
     for( int i = 0; i < generations; i++ ) {
        population.evolve();
     }

      long endTime = System.currentTimeMillis();
     System.out.println("\n"+"Total optimization time: " + (endTime - startTime)+ " ms");
     ...
}
```

3.1 Construction of GA chromosome

For the GA optimization process some of defined parameters of theoretical model can be fixed (by selection in a table of fixed parameters) and parameters released for optimization are then assigned to genes of constructed chromosome. In previous listing void solveGA(.) receives information about fixed parameters in boolean[] fixedParams. Then array fixedParams is used for the determination of number of genes and construction of chromosomes:

```
    //set number of genes:
     int geneCount = (int) fixedParams.length;
     for(int r=0; r<fixedParams.length; r++){
        if (fixedParams[r]) {geneCount--;}
     }
    //genecount = the number of genes, representing released parameters, max
fixedParams.length

    //allocate genes:
     Gene[] mGene = new Gene[geneCount];
     int geneIndx = 0;
     for(int r=0; r< parametreModelu.length; r++){
        if (!fixedParams[r]) {
          //use structure DoubleGene(configuration, minBound, maxBound), double precision
          //delta = permitted interval for modification of suggested variable, percent
          try {
                mGene[geneIndx] = new DoubleGene(conf, parametreModelu[r]-
                delta*parametreModelu[r]/100,
                parametreModelu[r]+delta*parametreModelu[r]/100);
                geneIndx++;
          }
          ...
```

In this definition a genes of chromosome are defined as double precision data type and are created only for parameters released for GA optimization. The size of the chromosome is therefore defined according to the number of released parameters. Parameter of theoretical model parametreModelu[r] represented by given gene is used also for determination of bound interval (minBound, maxBound) defining the interval of acceptable change of parametreModelu[r] value. We use special parameter *delta* defined in range (0,100) for determination of the bound interval as percentage of the parametreModelu[r] value. Value

delta is taken from an array parametreModelu[68]. User defined parameters for the GA optimization are taken from parametreModelu[60] (number of evolution steps) and parametreModelu[61] (number of chromosomes in a population). Information about inserting of the fittest chromosome into new population (elitism) is provided to the JGAP Configuration object by conf.setPreservFittestIndividual(true) statement.

3.2 Computation of fitness

The name of the fitness function (*fitnesFunkcia*) is provided to the Configuration object in a statement conf.setFitnessFunction(fitnesFunkcia). In our JGAP implementation fitnesFunkcia is defined in a public class *modelFitness.java*. This class extends FitnessFunction class of JGAP. From given chromosome it reconstructs (in public double evaluate(.)) the values of parameters coded in genes of proposed chromosome and calls getActualFitness(.). This is illustrated in Listing 2.

Listing 2.

```
public double evaluate(IChromosome chromParametre, double[] parametre, double[]
wavelength,  double[] experimentalData, double[] sigma, boolean[] fixedParams){

    for(int r=0; r<this.fixedParams.length; r++){
      if (!this.fixedParams[r])
     {this.parametre[r]=((Double)
chromParametre.getGene(g).getAllele()).doubleValue();}
      }
fitnessE=getActualFitness(

this.parametre,this.wavelength,this.experimentalData,this.sigma,this.fixedParams);

return fitnessE;
}
```

Public double getActualFitness(this.parametre, this.wavelength, this.experimentalData, this.sigma, this.fixedParams) receives in *this.parametre* a set of parameters for reconstruction of theoretical model of spectral reflectance. These values are proposed by the GA for testing of improvement of theoretical model. In getActualFitness(.) the value of proposed model fitness is computed by using Eq. (28), with passed experimental spectral reflectance in *experimentalData* at wavelengths passed in *wavelength* with dispersion *sigma*.

4. VIMSO method application: study of optical properties of amorphous silicon thin films

Undoped amorphous silicon thin films passivated by hydrogen are important for the applications in photovoltaics and optoelectronics. Plasma-enhanced chemical vapour deposition (PECVD) and hot-wire assisted chemical vapour deposition are techniques often used to deposit amorphous silicon thin films (a-Si). Amorphous a-Si thin films suffer from light-induced metastability of the microscopic origin. In optical applications based on

hydrogenated amorphous silicon, control of the optical properties is crucial to obtain well functioning devices.
Thin films deposited from hydrogen diluted silane plasma (a-Si:H) have improved stability against prolonged light soaking when compared with films deposited from pure silane (SiH_4). Hydrogen plays a central role in modifying the electrical and optical properties of amorphous Si for the photovoltaic and optical sensor applications. It is important to have a-Si:H with high optical absorption and with high content of hydrogen in the material to get sufficient electrical quality. The introduction of hydrogen modifies the silicon layer structure by changes in short and intermediate-range order (network bond-length and angle distributions). The presence of Si-H bonds also results in the creation of new states in the electron and phonon densities of states and in modifications of densities of electronic and vibrational states of Si. We have examined a series of a-Si:H films grown under varying PECVD deposition conditions with different hydrogen dilution, the film thickness or the substrate material. Material properties are strongly dependent on the deposition conditions and therefore a systematic investigation of sample properties connected with these deposition and passivation procedures is necessary. In this part we shall describe results, obtained by implementation of VIMSO method for determination of optical properties of the a-Si:H thin films deposited on glass from hydrogen diluted silane plasma.

4.1 Experiment

Hydrogenated amorphous silicon (a-Si:H) films have been deposited under a wide range of deposition conditions on a Corning 1737 glass substrates by 13.5 MHz rf excited parallel plate PECVD deposition system (Müllerová, 2005). The rf power was 13.5 W, the substrate temperature 194 °C and the total chamber pressure 200 Pa. The samples were deposited from the hydrogen (H_2) diluted silane (SiH_4) plasma under varied H_2/SiH_4 gas flows (the dilution D). The sample series deposited under varying dilution is described in a Table 1. All the samples were prepared with approximately the same thickness (~ 400 nm) to avoid the film thickness influence on the sample properties.

sample	dilution D	thickness [nm]	rms roughness [nm]
s1	0	390	-
s2	10	394	0.756
s3	20	385	1.013
s4	30	388	3.629
s5	40	402	5.476
s6	50	397	5.021

Table 1. Samples under study.

UV-VIS spectral reflectance measurements were performed with Pye Unicam/Philips PU 8800 spectrophotometer in the single beam mode with 2 nm slit at nearly normal incidence and at room temperature. The spectral region was set to (300 – 800) nm The probed sample areas were ~ 0.2 cm^2. A freshly evaporated aluminium sample was used for the reference reflectance data collection. Surface roughness was measured by the atomic force microscope NT - MDT SPM Solver P7 LS operating in the contact repulsive mode using a silicon tip cantilever. The lateral resolution of AFM measurements was ~ (1 – 2) nm, the vertical

resolution 0.01 nm. Standard rms roughness values were determined from the measured surface height function at area (2 x 2) μm^2 . Experimental spectral reflectances of a-Si:H thin films are shown in Fig. 9.

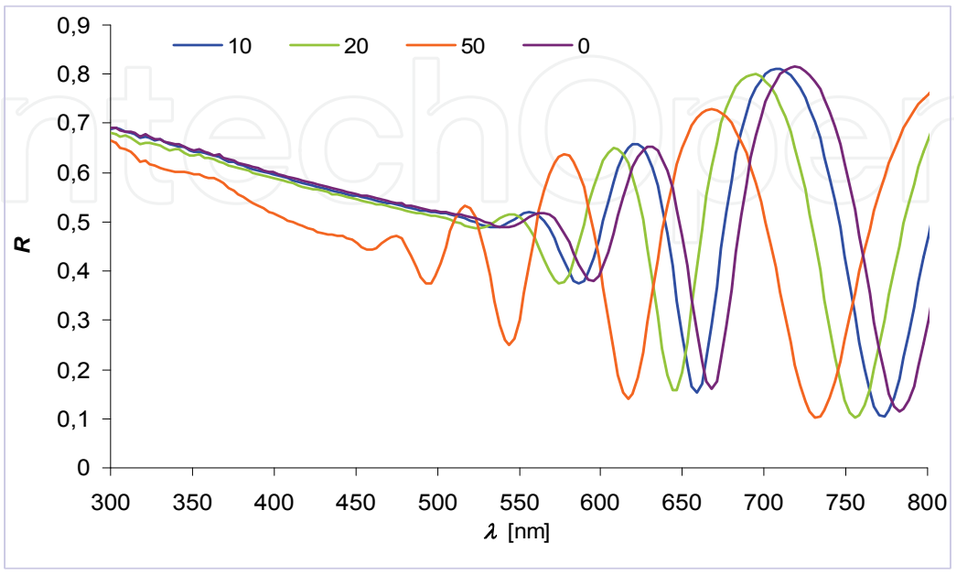

Fig. 9. Experimental spectral reflectances *R* of a-Si:H thin films prepared with hydrogen dilution D = 0, 10, 20, 50.

4.2 Theoretical model of a-Si:H thin film reflectance

The VIMSO method is based on two step optimization procedure, used for the construction and refinement of theoretical model of the spectral reflectance or trasmittance of the analysed structure. In the first step the microstructural model of the layered system is constructed in graphical interface. Here the materials, thickness and homogeneity of individual layers are defined and the initial estimation of theoretical model variables is obtained. In our approach a set of dispersion relations commonly used for the determination of optical properties of semiconductor and dielectric materials is implemented. The values of the theoretical model variables are modified interactively and temporary defined theoretical model is graphically compared to the experimental data. Simultaneously the numerical value of the χ^2 value defined by Eq.(28) is used as a goodness of fit measure. Proposed structural model describing the optical and structural properties of investigated samples is shown in Fig. 10. It consists of the overlayer, a-Si:H and transition layer on a glass substrate.

In the following step the values of theoretical model parameters are numerically refined by the genetic algorithm. In our implementation the environment for the GA optimization is interactively modified (the probabilities of the genetic operators, number of chromosomes in population, number of populations, maximal interval for changing selected value, and other). It is possible to fix some selected parameters and not allow the GA to change these fixed values. This enables avoiding the influence of the mutual correlation of theoretical model variables onto the convergence properties of the optimization process and

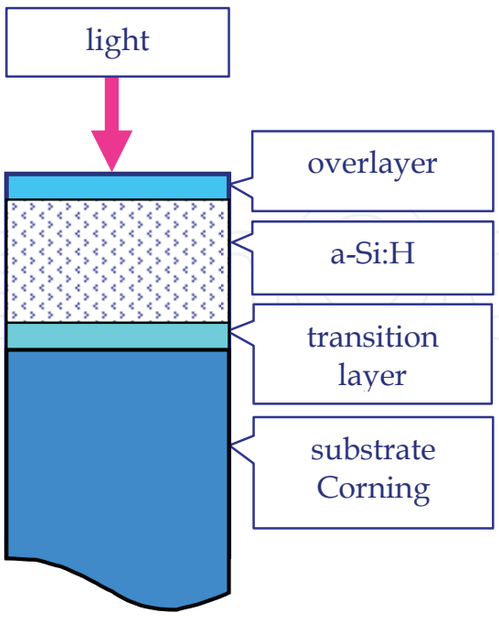

Fig. 10. Structural model proposed for analysis of optical properties of a-Si:H thin films.

implementation of the subjective decisions concerning the importance of individual variables for the problem solution. This combination of visual modeling followed by the stochastic optimization of theoretical model speeds up the solution of the structure theoretical model. The set of possible dispersion relations contains analytical models, derived by the quantum theory of interaction of light and matter as well as phenomenological equations and experimentally obtained data were implemented.
For the description of the spectral dependency of the refractive index n and the extinction coefficient κ of amorphous a-Si:H layer we proposed a simple polynomial model

$$n(\lambda) = \sum_{i=0}^{6} a_i \lambda^i, \ \kappa(\lambda) = \sum_{j=0}^{6} b_j \lambda^j, \ a_i, b_j \in R \,. \tag{29}$$

The optical properties of overlayer and transition layer are described by a Bruggeman model of the effective media approximation with the fraction f of the embedded phase

$$f \frac{\varepsilon_1 - \varepsilon_{eff}}{\varepsilon_1 + 2\varepsilon_{eff}} + (1 - f) \frac{\varepsilon_2 - \varepsilon_{eff}}{\varepsilon_2 + 2\varepsilon_{eff}} = 0 \,, \tag{30}$$

where $\varepsilon_1, \varepsilon_2, \varepsilon_{eff}$ are permitivities of the embedded phase, of a matrix material and resulting effective permitivity of the a-Si:H layer respectively. The overlayer is used to account for the natural oxide layer influence and the transition layer describes local changes of the optical properties at the a-Si:H/glass substrate interface. The ambient is air and the substrate is Corning 1737 glass. Theoretical spectral reflectance R_{theor} of proposed structural model is computed from multilayer reflection coefficients by equation Eq.(23-24).
The theoretical spectral reflectance of the whole structure is corrected for the surface roughness by the equation

$$R_{corr}(\lambda) = R_{theor}(\lambda)\frac{c_1}{1+\frac{c_2}{\lambda}}, \tag{31}$$

where c_1 and c_2 are real constants. Theoretical model of spectral reflectance $R_{corr}(\lambda)$ contains in this approach 20 unknown parameters: $a_0,\ldots,a_6,b_0,\ldots,b_6,c_1,c_2,f,d_1,d_2,d_3$.

4.3 Results

Resulting theoretical model of spectral reflectance for sample s3 obtained by the VIMSO method is in Fig. 11. Similar results were obtained also for other analysed samples. Refractive indices and extinction coefficients reconstructed from $R_{corr}(\lambda)$ models are in Fig. 12 and Fig. 13.

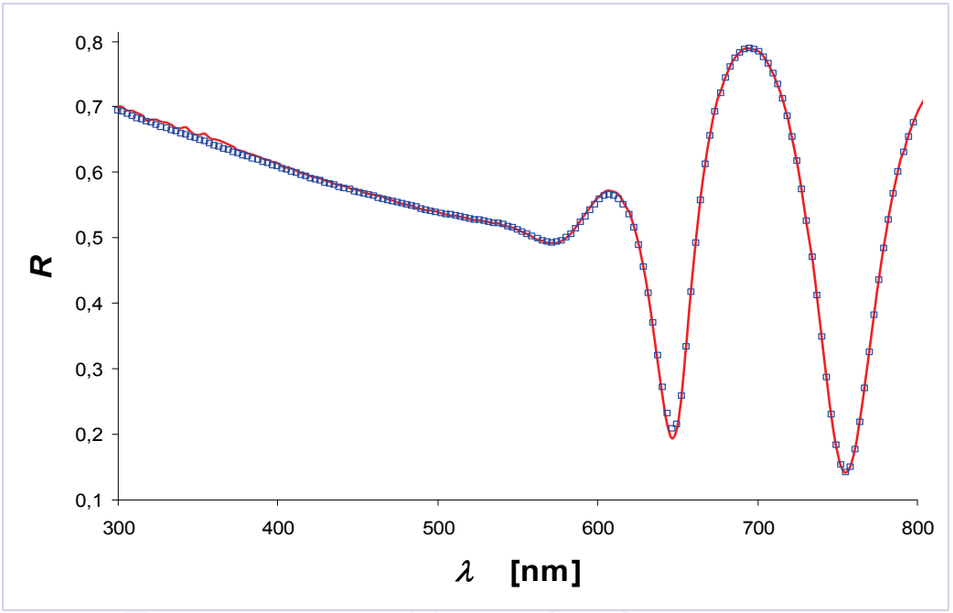

Fig. 11. Fit of theoretical model of spectral reflectance of sample s3 (blue squares), and experimental reflectance function (red line).

By using of proposed theoretical model the spectral reflectance function can be modeled in agreement with the experimental data.

The size of the surface structural objects measured by the AFM increases with increasing dilution. We suppose that with increasing dilution D the a-Si:H structure becomes polycrystalline. The samples prepared at the dilution under 20 remain amorphous. The films prepared at D ≥ 30 show polycrystalline features. The protocrystalline regime occurs between the dilutions 20 and 30. Reduction of the refractive index and extinction coefficient of a-Si:H layers with increasing dilution can be explained by the development of a void fraction in the structure. These voids are created under hydrogenation and creation of the polycrystalline phase. Remarkable changes of the optical properties connected with these processes can be observed under dilution D ≥ 30 as can be seen in Fig. 12 and Fig. 13.

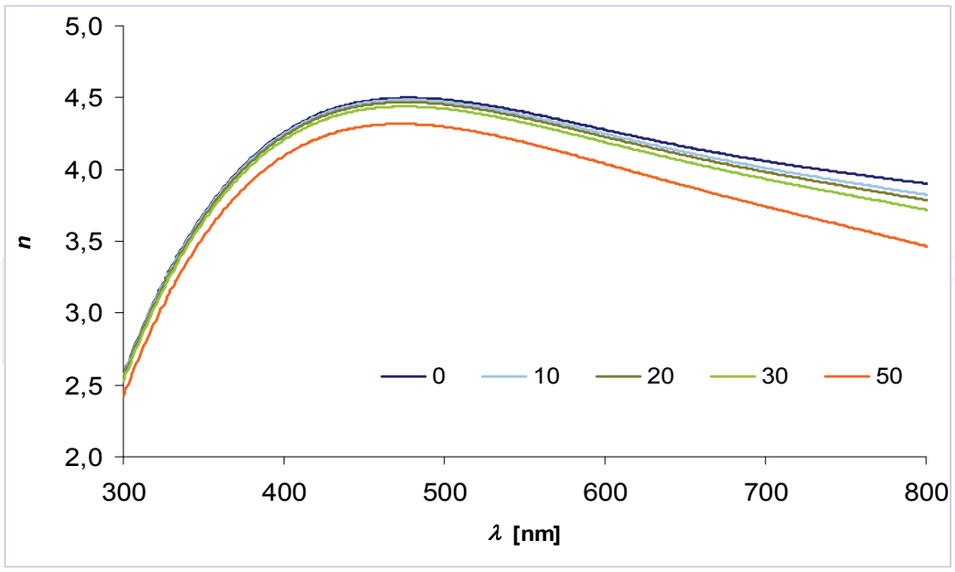

Fig. 12. Reconstructed spectral refractive indices of a-Si:H thin films.

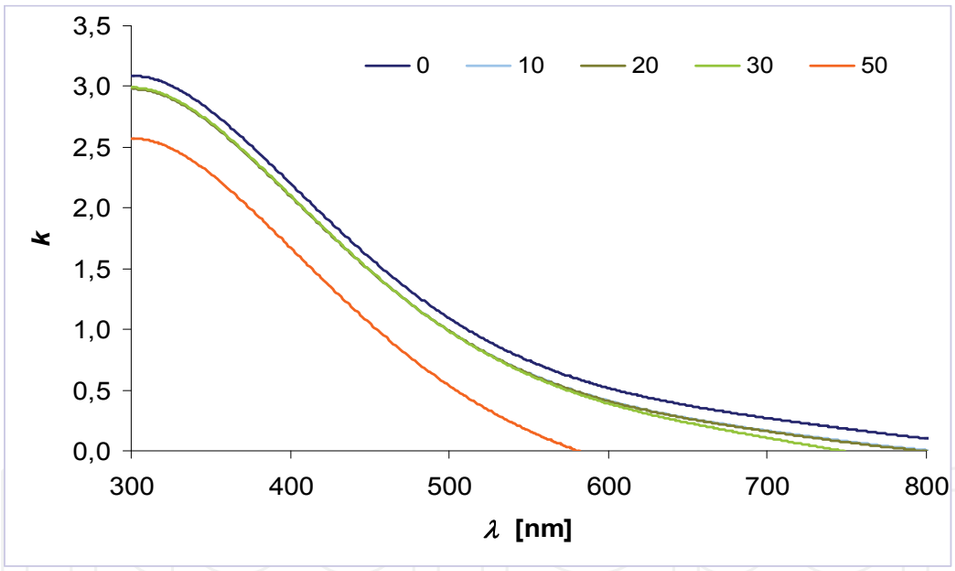

Fig. 13. Reconstructed spectral extinction coefficients of a-Si:H thin films.

5. Conclusion

Theoretical model of physical system is constructed in our approach in two steps. Microstructural and optical properties of multilayer system are proposed in visual environment and then the initial estimation of model parameters is refined by the genetic algorithm. It enables comfortable modification of proposed theoretical model, incorporating of subjective criteria, testing of mutual correlation of model parameters and control of convergence abilities of resulting numerical model. The VIMSO method is implemented in

JAVA language in NET Beans IDE. For the GA optimization of estimated numerical model the JAVA JGAP package is used. It is based on object-oriented programming and provides all benefit from this property – implementation of data abstraction, modularity, encapsulation and inheritance. It is possible to define special chromosomes and fitness function suitable for solving of specified problem. By using of the VIMSO method adequate description of experimental spectral reflectance of semiconductor thin film samples was reached. It is supported by implementation of several dispersion models for semiconductors and dielectrics, suitable effective media approximation models, surface roughness correction, and by the "user friendly" philosophy applied to building of the layer structure and modification of model variables.

Changes in optical properties of real a-Si:H thin films due to the increasing hydrogen dilution were analysed by optimising of the spectral reflectance theoretical model. Proposed microstructural and dispersion theoretical model was successfully optimised by comparison to the experimental data. Development of the spectral index of refraction and extinction coefficient with change of the deposition conditions was obtained. Changes in optical properties of a-Si:H samples determined by using the VIMSO method provide reliable tool for making conclusions about development of the material structure and about interaction of light and prepared optical media.

Beside of the refractive index and extinction coefficient a set of other important parameters describing the structure and optical properties can be extracted from fitted theoretical model. Very useful is information about the thicknesses of individual layers, influence of the effective media approximation, connection of surface roughness and spectral reflectance and other parameters extracted from the resulting fit. The combination of visual estimation of initial theoretical model and refinement of this estimation by the genetic algorithm is suitable tool for modeling of complex physical systems. It enables reliable incorporation of new phenomena into theoretical model in order to explain the experimental data. When solving this task correlated parameters can be easily fixed and suitable restrictions of remaining parameters can be effectively implemented.

6. References

Abeles, F. (1950). *Recherches sur la propagation des ondes electromagnetiques sinusoidales dans les milieux stratifies. Application aux couches minces*. Annales de Physique. Paris.

Born, M. & Wolf, E. (1975). *Principles of Optics*. Pergamon Press, London.

Bury, P.; Hockicko, P.; Jurečka, S. & Jamnický, J. (2004). Analysis of Acoustic Attenuation Spectra Due to Ion Transport Processes in Glassy Electrolytes. *Physica Status Solidi*. No. 11, 2004, pp. 2888-2891.

Coley, D., A. (1999). *An introduction to genetic algorithms for scientists and engineers.* World Scientific Publishing Co., Singapore.

Furman, S., A. & Tikhonravov, A., V. (1992). *Basics of optics of multilayer systems*. Edition Frontieres, Gif-sur-Yvette, Paris.

Hawlitzek, F. (2000). *Java 2*. Adsdison-Wesley Verlag, München, Germany.

Hecht, E. (2002). *Optics*, Addison Wesley, San Fransisco.

Chen, Y., F.; Kwei, C., M. & Tung, C., J. (1993). Optical-constants model for semiconductors and insulators. *Physical Review B*. Vol. 48, No. 7, 1993, pp. 4373-4379.

JGAP http://jgap.sourceforge.net/index.html

Jurečka S.; Havlík M. & Jurečková M. (2004). Genetická syntéza difrakčného profilu. *Advances in Electrical and Electronic Engineering,* Vol. 3, No. 1, 2004, p. 27-30.

Koza, J. R. (1992). *Genetic Programming: On the Programming of Computers by Means of Natural Selection*. Massachusetts Institute of Technology, USA.

Lekner, J. (1987). *Theory of reflection*. Martinus Nijhoff Publishers, Dordrecht, The Netherlands.

Mallet, P.; Guérin, C., A. & Sentenac, A. (2005). Maxwell-Garnett mixing rule in the presence of multiple scattering: Derivation and accuracy. *Physical Review* B 72, 014205, 2005.

Müllerová, J.; Jurečka, S., Šutta, P. & Mikula, M. (2005). Structural and optical studies of a-Si:H thin films: from amorphous to nanocrystalline silicon. *Acta Physica Slovaca*, Vol. 55, No. 3, 2005, pp. 351-359.

Roussel, P., H.; Vanhellemont, J. & Maes, H., E. (1993). Numerical aspects of the implementation of effective-medium approximation models in spectroscopic ellipsometry regression software. *Thin Solid Films*, Vol. 234, 1993, pp. 423-427.

Sihvola, A. (1999). *Electromagnetic Mixing Formulas and Applications*. The Institution of Electrical Engineers, New York.

SUN http://www.oracle.com/us/sun/index.html

Tompkins, H., G. & Irene, E., A. (2005). *Handbook of ellipsometry*. Springer Verlag, ISBN 3-540-22293-6, Heidelberg.

Weiglhofer, W. S. & Lakhtakia, A. (2003). *Introduction to complex mediums for optics and electromagnetics*. SPIE, Bellingham, USA.

IntechOpen

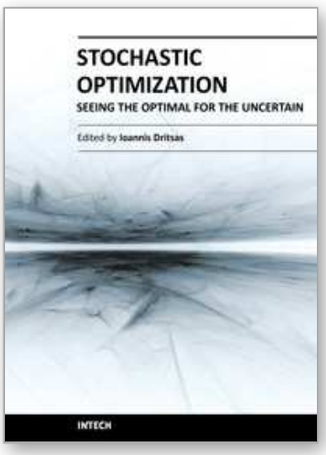

Stochastic Optimization - Seeing the Optimal for the Uncertain
Edited by Dr. Ioannis Dritsas

ISBN 978-953-307-829-8
Hard cover, 476 pages
Publisher InTech
Published online 28, February, 2011
Published in print edition February, 2011

Stochastic Optimization Algorithms have become essential tools in solving a wide range of difficult and critical optimization problems. Such methods are able to find the optimum solution of a problem with uncertain elements or to algorithmically incorporate uncertainty to solve a deterministic problem. They even succeed in â€œfighting uncertainty with uncertaintyâ€. This book discusses theoretical aspects of many such algorithms and covers their application in various scientific fields.

How to reference
In order to correctly reference this scholarly work, feel free to copy and paste the following:

Stanislav Jurečka (2011). Theoretical Model of the Physical System: Optimization by the Genetic Algorithm, Stochastic Optimization - Seeing the Optimal for the Uncertain, Dr. Ioannis Dritsas (Ed.), ISBN: 978-953-307-829-8, InTech, Available from: http://www.intechopen.com/books/stochastic-optimization-seeing-the-optimal-for-the-uncertain/theoretical-model-of-the-physical-system-optimization-by-the-genetic-algorithm

INTECH
open science | open minds

InTech Europe
University Campus STeP Ri
Slavka Krautzeka 83/A
51000 Rijeka, Croatia
Phone: +385 (51) 770 447
Fax: +385 (51) 686 166
www.intechopen.com

InTech China
Unit 405, Office Block, Hotel Equatorial Shanghai
No.65, Yan An Road (West), Shanghai, 200040, China
中国上海市延安西路65号上海国际贵都大饭店办公楼405单元
Phone: +86-21-62489820
Fax: +86-21-62489821

© 2011 The Author(s). Licensee IntechOpen. This chapter is distributed under the terms of the Creative Commons Attribution-NonCommercial-ShareAlike-3.0 License, which permits use, distribution and reproduction for non-commercial purposes, provided the original is properly cited and derivative works building on this content are distributed under the same license.

IntechOpen

IntechOpen